Marine Pollution Bulletin 231 (2026) 119952

Contents lists available at ScienceDirect

Marine Pollution Bulletin

journal homepage: www.elsevier.com/locate/marpolbul

Stage-specific metabolic responses in blue mussels to marine shipping-related acoustic and chemical stressors☆

Stéphane Beauclercq [a,*], Delphine Veillard [b], Richard Saint-Louis [b], Frédéric Olivier [c,d], Dror E. Warschawski [e], Réjean Tremblay [b], Isabelle Marcotte [a,*]

[a] Department of Chemistry, Université du Québec à Montréal, P.O. Box 8888, Downtown Station, Montreal, QC, Canada
[b] Institut des Sciences de la Mer de Rimouski, Université du Québec à Rimouski, Rimouski, QC, Canada
[c] Laboratoire de 'Biologie des Organismes et Écosystèmes Aquatiques' (BOREA), Muséum national d'Histoire naturelle, Sorbonne Université, Université des Antilles, Centre National de la Recherche Scientifique, Institut de Recherche pour le Développement, 207, CP53, 61 rue Buffon, 75005, Paris, France
[d] Université Bretagne Occidentale (UBO), CNRS, IRD et Institut Universitaire Européen de la Mer, 29280, Plouzané, France
[e] Chimie Physique et Chimie du Vivant, CPCV, CNRS UMR 8228, Sorbonne Université, École normale supérieure, PSL University, 75005, Paris, France

ARTICLE INFO

Keywords:
Shipping noise
Pollution
Oceans
Mussel
Larvae
Metabolism
^{1}H NMR-based metabolomics

ABSTRACT

Maritime traffic exposes coastal organisms to both acoustic disturbance and chemical pollution, yet how these stressors affect and interact across early developmental stages remains poorly understood. We investigated stage-specific metabolic responses of blue mussel (*Mytilus edulis*) larvae to shipping-related noise, chemical pollution, and their combination using untargeted nuclear magnetic resonance-based metabolomics. Metabolic profiles were analysed in D-larvae and post-larvae exposed to noise or chemical pollution, as well as in post-larvae originating from chemically exposed embryos and subsequently subjected to acoustic stress during metamorphosis.

During embryogenesis, acoustic and chemical stressors elicited largely overlapping metabolic responses, primarily involving modulation of free amino acid pools and nitrogen-related pathways. In contrast, post-larvae exhibited distinct, stressor-specific metabolic signatures. Acoustic exposure was associated with increased metabolic turnover and mobilisation of energetic substrates, whereas embryonic chemical exposure resulted in persistent metabolic constraints during metamorphosis, reflected in energy balance and membrane-associated metabolites. In post-larvae originating from chemically exposed embryos and subsequently exposed to shipping noise during metamorphosis, metabolic profiles closely resembled those induced by chemical stress alone, indicating persistent carry-over effects of embryonic chemical exposure.

Together, these results demonstrate that developmental stage strongly modulates metabolic sensitivity to shipping-related stressors and that early-life chemical exposure can shape metabolic plasticity at later life stages.

1. Introduction

Maritime transport affects marine ecosystems through both acoustic disturbance and chemical contamination. Underwater noise (Chauvaud et al., 2018), together with the release of hydrocarbons, metals, and antifouling compounds (Byrnes et al., 2020), is an increasingly significant source of stress for coastal ecosystems. Expanding marine activities, including commercial shipping, oil and gas exploration and operation, offshore wind farms and other renewable energy devices, dredging, and harbor constructions, intensify these pressures and increasingly overlap with productive coastal habitats (Halpern et al., 2015). In particular, underwater noise generated by shipping vessels has become a dominant component of the low-frequency marine soundscape, as they account for more than 90% of anthropogenic acoustic input in the ocean (Chauvaud et al., 2018). Vessel noise has increased more than thirty-fold in some parts of the ocean (e.g., the Northeast Pacific) over the last 50 years and continues to rise with global maritime traffic (Jalkanen et al., 2022; McDonald et al., 2006). Large ships generate predominantly low-frequency sounds reaching 160–220 dB re 1 μPa, which can propagate hundreds of kilometres (Duarte et al., 2021; Richardson Jr et al., 2013).

☆ This article is part of a Special issue entitled: 'OD-Pollution and Health MPB' published in Marine Pollution Bulletin.

* Corresponding authors.
E-mail addresses: beauclercq.stephane@uqam.ca (S. Beauclercq), marcotte.isabelle@uqam.ca (I. Marcotte).

https://doi.org/10.1016/j.marpolbul.2026.119952
Received 19 March 2026; Received in revised form 28 May 2026; Accepted 30 May 2026

Sea transport is also an important source of chemical oceanic contamination. Vessel operations contribute to the release of heavy metals, hydrocarbons, and other contaminants through bilge water discharge, antifouling coatings, and spills (Calgaro et al., 2025). These compounds can accumulate in coastal waters and sediments, where they disrupt marine organisms metabolism, such as filter feeders, through absorption and bioaccumulation (Mearns et al., 2015; Svavarsson et al., 2021). Because acoustic and chemical stressors associated with shipping often co-occur, marine organisms are frequently exposed to multiple pressures simultaneously, yet their combined effects remain poorly characterized (Crain et al., 2008).

The biological effects of shipping noise depend on exposure intensity, frequency, duration, and include physiological stress, metabolic disruption, impaired development, and behavioural changes across marine species (Blom et al., 2019; de Soto et al., 2016; Lillis et al., 2016; Masud et al., 2020). While most research on underwater noise has focused on fishes and marine mammals due to their specialized auditory organs (Erbe et al., 2019; Popper and Hawkins, 2019), invertebrates are also sensitive to particle motion generated by vessel noise and to chemical contamination of their environment (Breitwieser et al., 2016; de Soto et al., 2016). Sessile bivalves are particularly exposed because they cannot avoid stressors and continuously filter large volumes of water (Hubert et al., 2022).

In mussels, shipping noise related stressors have been linked to DNA damage, altered physiological performance, and biochemical changes in tissues and haemolymph (Solé et al., 2023). Recent laboratory studies have further demonstrated that vessel noise induces coordinated behavioural and biochemical responses, including changes in valve-gaping activity and oxidative stress biomarkers (El-Dairi et al., 2026). Chemical contaminants associated with maritime activity are also known to disrupt metabolic pathways and redox balance in bivalves (Cappello et al., 2013a; Lehtonen et al., 2006; Regoli and Giuliani, 2014). However, comparatively little is known about how these stressors affect early life stages that are critical for recruitment and aquaculture production. Emerging evidence suggests that vessel noise (Jolivet et al., 2016; Veillard et al., 2025a, 2025b) and chemical pollution (Veillard et al., 2026) can influence larval development, metabolism, and settlement in mussels, but the underlying metabolic responses, particularly under combined acoustic and chemical exposure, remain insufficiently described.

The blue mussel (*Mytilus edulis*) is a key species in coastal ecosystems and an important aquaculture resource in the Northwestern Atlantic. Beyond its economic value, it contributes to ecosystem functioning through phytoplankton filtration and nutrient cycling (Kotta et al., 2020; van der Schatte Olivier et al., 2021). To address current gaps in knowledge regarding early-stage sensitivity to shipping-related pollution, this study examines the metabolic responses of mussels, a key coastal species, during embryogenesis and metamorphosis to acoustic stress, chemical pollution, and sequential combined exposure involving embryonic chemical exposure followed by acoustic exposure during metamorphosis under the controlled conditions of mesocosms using untargeted ^{1}H-nuclear magnetic resonance (NMR)-based metabolomics.

2. Materials and methods

2.1. Experimental set-up

Blue mussel (*Mytilus edulis*) embryos and pediveliger larvae were exposed to three levels of shipping-related stressors and a control using *Larvosonic* mesocosms, engineered to emit sounds with minimal reverberation and resonance (Olivier et al., 2023). Acoustic and chemical exposures were conducted either independently or sequentially, depending on the treatment.

Adult blue mussels (*Mytilus edulis*; 50–60 mm shell length) originating from St. Peters Bay, Prince Edward Island, Canada (46.4295°N, 62.6603°W), were induced to spawn individually using a 10 °C thermal shock following natural gonad maturation, as previously described (Rayssac et al., 2010; Veillard et al., 2026, 2025a, 2025b). Fertilization was performed in UV-treated ultrafiltered seawater at 18 °C using a ratio of 10 spermatozoids per egg. Larvae were maintained under controlled conditions (18 °C, salinity 23–24 PSU, photoperiod 15 h light : 9 h dark). During larval rearing and post-larval experiments, organisms were fed every 2 days with a mixed microalgal diet composed of *Pavlova lutheri*, *Tisochrysis lutea*, *Chaetoceros muelleri*, *Tetraselmis suecica*, and *Nannochloropsis oculata*, as previously described in (Veillard et al., 2025a).

2.1.1. Acoustic exposure

Acoustic experiments were conducted in four *Larvosonic* mesocosms, each comprising six independent 5-L cylinders containing approximately 25,000 embryos or pediveliger larvae per cylinder. Playback consisted of an 80-min looped soundtrack of cargo ship noise (Nohlan Ava, 120 m), recorded in Saint-Pierre-et-Miquelon (France) between November 2020 and April 2021 (Veillard et al., 2025a). The sequence included ship arrival (11 min), a simulated handling break (39 min), departure (8.5 min), and a silent period (21.5 min), and is representative of the acoustic signature of commercial vessels (McKenna et al., 2012).

Organisms were exposed either until the D-larval stage (early veliger) or until the post-larval stage (spat, following metamorphosis and substrate attachment) (Fig. 1). D-larval and post-larval acoustic experiments were replicated one and three times, respectively. Acoustic treatments consisted of ambient sound (116 ± 1 dB re 1 μPa) and three increasing noise levels: low (121 ± 4 dB re 1 μPa), medium (127 ± 2 dB re 1 μPa), and high (151 ± 2 dB re 1 μPa). These levels corresponded, under field conditions, to approximate distances of 1.8 km, 735 m, and 18.5 m, respectively, from the noise source in the Saint-Pierre and Miquelon archipelago (Veillard et al., 2025a).

Acoustic calibration of the *Larvosonic* mesocosms, including hydrophone measurements, speaker positioning, resonance/reverberation analyses, sound pressure characterization, and particle motion measurements, was previously described in detail by Olivier et al. (2023). Briefly, underwater speakers were positioned centrally within each mesocosm and calibrated hydrophones were used to characterize sound pressure levels and power spectral densities (PSD) across treatments. The ambient sound level measured in the control treatment corresponded to the residual background acoustic conditions within the *Larvosonic* system during silence playback rather than pristine open-ocean ambient noise. Previous characterization of the Larvosonic system showed that background acoustic conditions in the control mesocosms were within the range reported for temperate coastal environments under variable wind conditions (Olivier et al., 2023). PSD analyses confirmed distinct acoustic profiles and increasing acoustic energy across the low, medium, and high shipping-noise treatments (Veillard et al., 2025a). Calibration of the *Larvosonic* system confirmed that sound pressure and particle motion scaled proportionally across treatments, ensuring consistent exposure gradients (Olivier et al., 2023).

2.1.2. Chemical pollution exposure

Chemical exposure experiments were conducted following the protocol described by Veillard et al. (2025a), using a contaminant cocktail representative of chemical pollution associated with industrial ports and maritime traffic. The mixture included copper (Cu), mercury (Hg), lead (Pb), and petroleum-derived hydrocarbons (diesel), selected based on concentrations measured in adult mussels and sediments from the port of Saint-Pierre-et-Miquelon (France).

Concentrations in the exposure medium were 4 $\mu g \bullet L^{-1}$ Cu^{2+}, 23 $\mu g \bullet L^{-1}$ Pb^{2+}, 0.05 $\mu g \bullet L^{-1}$ Hg^{2+}, and 0.01 $\mu g \bullet L^{-1}$ dissolved hydrocarbons. These concentrations were calculated using bioconcentration factors in adult blue mussels to reflect environmentally realistic exposure levels associated with shipping activity (Veillard et al., 2026). For the D-larval experiment, embryos originating from the second spawning event performed in early July (Veillard et al., 2026) were exposed continuously to the contaminant cocktail from fertilization until the D-

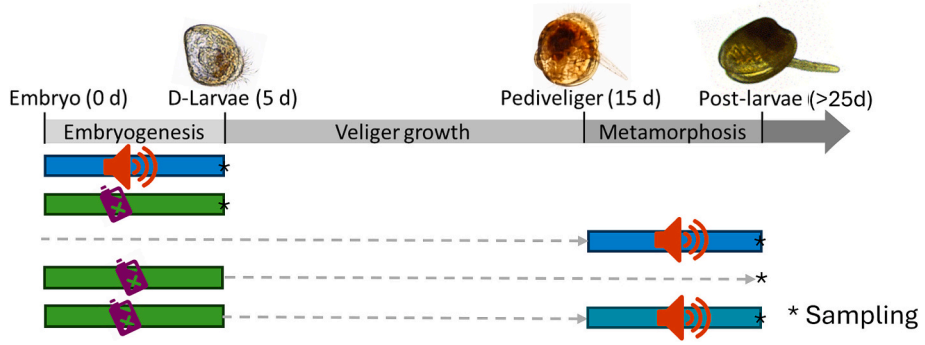

Fig. 1. Experimental design and sampling strategy across developmental stages. Blue mussel (*Mytilus edulis*) larvae were exposed during embryogenesis or metamorphosis to acoustic stress (blue bar), chemical pollution (green bar), or sequential combined exposure involving embryonic chemical exposure followed by acoustic exposure during metamorphosis (teal bar) at two developmental stages. Larvae were collected at the D- or post-larval stages for metabolomics analysis. (For interpretation of the references to colour in this figure legend, the reader is referred to the web version of this article.)

larval stage. For the post-larval experiment, embryos were exposed to the contaminant cocktail from fertilization to the D-larval stage and subsequently reared in clean seawater until the post-larval stage (Fig. 1).

2.1.3. Sequential combined exposure

Sequential combined exposure experiments involved embryonic chemical exposure followed by acoustic exposure during metamorphosis. As part of the sequential exposure design, embryos were exposed to the contaminant cocktail from fertilization to the D-larval stage and then reared in clean seawater until the pediveliger stage. Pediveliger larvae were subsequently transferred to the *Larvosonic* mesocosms and exposed to the same acoustic treatments described above until post-larval stage (Fig. 1).

2.1.4. Sampling and storage

At the end of noise exposure, D-larvae or post-larvae were sieved (20 μm or 100 μm mesh), flash-frozen in liquid nitrogen, freeze-dried, and stored at −80 °C until metabolomic analysis. Detailed rearing and experimental treatment conditions are reported elsewhere (Veillard et al., 2026, 2025a, 2025b).

2.1.5. Experimental replication

The study was conducted as three independent experimental runs, each based on separate larval rearing batches. In all experiments, the independent biological replicate was the *Larvosonic* cylinder. Larvae were pooled within each cylinder to obtain sufficient biomass for extraction and ^{1}H NMR analysis, while preserving replicate-level independence at the cylinder level. The first experiment (July 2021) evaluated acoustic exposure (ambient sound control vs. shipping-noise treatments) and produced both D-larvae and post-larvae samples (Veillard et al., 2025a, 2025b). The two other experiments (June or July 2022) evaluated the impact of chemical pollution during embryogenesis (Veillard et al., 2026) and, for post-larvae, included acoustic exposure during metamorphosis either alone or following embryonic chemical exposure.

The untargeted ^{1}H NMR approach applied here was the only analytical platform common to all experimental runs and developmental stages, thereby providing an integrative overview of metabolic responses to acoustic and/or chemical stressors. This strategy complements previously published targeted LC–MS/MS metabolite profiling by enabling a broader, non-biased assessment of metabolic alterations.

For post-larvae, samples corresponding to identical treatment definitions were combined across experimental runs prior to multivariate modelling. Noise-only samples (no chemical exposure) from Experiments 1–3 were pooled within each acoustic exposure level, whereas chemical-only and sequential combined noise + chemical samples from experiments 2 and 3 were pooled within their respective treatment groups. All post-larval samples were processed using identical extraction, NMR acquisition, and post-processing procedures. The number of independent biological replicates per treatment and experimental run is provided in Table S1.

2.2. Larvae and tissues extraction for solution ^{1}H NMR

Freeze-dried larval pools (0.38 ± 0.27 mg D-larvae; 2.97 ± 0.83 mg post-larvae) were homogenized in microtubes using a micropestle. Metabolites were extracted following a modified Folch protocol (Folch et al., 1957) with a methanol/chloroform/water ratio of 2:2:1.4. Sequential additions of methanol/chloroform (2:1), chloroform, and water were performed, each followed by 30 s vortexing and a final 10 min sonication on ice (Branson 2510 sonicator, Branson Ultrasonics, Brookfield, CT, USA). Extracts were centrifuged (10,000 ×*g*, 10 min, 4 °C) to separate polar and lipophilic phases. The extractions were repeated three more times and the polar extracts were pooled before solvent evaporation in a SpeedVac (Thermo Fisher Scientific) at room temperature and stored at −80 °C until NMR analysis.

2.3. NMR spectroscopy, spectra post-processing, and assignment

Prior to acquisition, D-larvae extracts were reconstituted in 50 μL of NMR buffer (0.2 M potassium phosphate buffer, pH 7.4, in 99.9% D_2O with 0.13 mM 3-(trimethylsilyl)propionic-2,2,3,3-d_4 acid [TSP]) and transferred to 1.7 mm tubes. Post-larvae extracts were dissolved in 500 μL of the same buffer and transferred to 5 mm tubes.

^{1}H NMR spectra were acquired at 298 K using a Bruker Avance II+ 800 MHz spectrometer equipped with a 1.7 mm "QCI" microcryoprobe and SampleJet autosampler (D-larvae) or a Bruker Avance III 600 MHz spectrometer with a room temperature Broad Band Fluorine observe probe (post-larvae). A NOESYPR1D sequence was employed, with repetition delays of 5 s or 10 s and mixing times of 80 ms or 50 ms for D-larvae or post-larvae, respectively. ^{1}H NMR spectra were collected with 512 or 1024 scans for D-larvae or post-larvae, respectively, with 64 k points over a 12 ppm spectral width. Water suppression was achieved by presaturation during the repetition delay and mixing time.

Free induction decays were zero-filled to 128 k and multiplied by a 0.3 Hz line broadening factor prior to Fourier transformation using NMRProcFlow software (Jacob et al., 2017). Spectra were referenced to TSP at 0 ppm. Manual bucketing excluded regions corresponding to water, glycerol, methanol, and buckets with a signal-to-noise ratio (S/N) < 3. Prior to statistical analysis, spectra were normalized to the total integral, emphasizing relative changes within the soluble metabolite pool, whereas weight-based normalization used in previous targeted mass spectrometry analyses of the same material (Veillard et al., 2026, 2025b) reflected absolute concentrations per unit biomass. Metabolites

were identified using Chenomx software (Chenomx Inc., Edmonton, Canada), the HMDB database (Wishart et al., 2022), and published mollusc metabolomics references (Aru et al., 2020; Frizzo et al., 2021). Representative ^{1}H NMR spectra shown in Fig. S1 were used solely for metabolite identification and illustration purposes and were annotated independently of the $S/N \geq 3$ filtering applied to the analytical dataset.

2.4. Multivariate statistics

Multivariate analyses were performed using SIMCA 17 (Sartorius Stedim, Göttingen, Germany). Prior to analysis, NMR data were scaled to unit variance. Orthogonal projection to latent structures discriminant analysis (OPLS-DA) was used to define latent stress-response axes summarizing major metabolic changes associated with environmental exposures.

OPLS-DA models were adjusted for acoustic stress (control vs. high-level noise exposure), for chemical pollution (control vs. chemically exposed samples), and for sequential combined acoustic and chemical stress. Post-larval samples were combined across experimental runs prior to modelling. Variables contributing weakly or inconsistently to the predictive component were iteratively excluded using variable importance in projection (VIP) values and regression coefficients as filtering criteria until stabilization of the latent structure was achieved through maximization of cumulative explanatory ability (R^2Y) and predictive ability (Q^2) values (Beauclercq et al., 2022). Model statistical significance was assessed using cross-validated analysis of variance (CV-ANOVA) (Eriksson et al., 2008), with $p < 0.05$ considered statistically significant. R^2Y and Q^2 values were used to evaluate the explanatory and predictive performance of the models, respectively, with Q^2 estimated through internal cross-validation procedures implemented in SIMCA. For acoustic stress, samples exposed to intermediate noise levels were subsequently projected onto the stabilized stress-response axis without contributing to model calibration. OPLS-DA was used as a supervised exploratory approach to structure multivariate metabolic responses and to identify variables contributing to the stress-response axes based on their loadings on the predictive component.

Contribution plots were used to visualize the direction and magnitude of metabolite contributions to the stress-response axes, allowing biological interpretation of the metabolic changes associated with each exposure. Only assigned features were displayed. When multiple NMR signals corresponding to the same metabolite were retained in the OPLS-DA model, their contributions were averaged to obtain a single metabolite-level contribution value.

2.5. Metabolite pathway enrichment analysis

To identify the most affected metabolic pathways, discriminant metabolites in the OPLS-DA models were analysed separately for each larval stage and stressor using metabolite set enrichment analysis (Xia and Wishart, 2010), implemented in MetaboAnalyst (v6.0; www.metaboanalyst.ca) (Pang et al., 2024). Enrichment analysis was performed using over-representation analysis (ORA) with the "pathway-associated metabolite sets" library, which contains 99 metabolite sets derived from human metabolic pathways. ORA was based on hypergeometric tests to evaluate whether a given metabolite set was represented more than expected by chance within the input metabolite list.

3. Results

3.1. Distinct metabolic responses of D-larvae to acoustic and chemical stressors

First, we compared the metabolic responses of *M. edulis* D-larvae to shipping noise and to chemicals by ^{1}H NMR. To characterize metabolic changes associated with high-level noise exposure in D-larvae, an OPLS-DA model contrasting ambient (control, $n = 6$) and high noise (n = 6) conditions was fitted (Fig. 2A; Table S2). This model contained one predictive and one orthogonal component and showed high explanatory and predictive performance ($R^2Y = 0.97$, $Q^2 = 0.94$). The model was statistically significant according to CV-ANOVA ($p = 2.36 \times 10^{-4}$). The predictive component captured the major metabolic variation associated with high noise exposure, defining an acoustic stress-response axis. Eleven annotated metabolites presented in Fig. 2C contributed to this axis. Samples exposed to low (n = 6) and medium ($n = 4$) noise levels were subsequently projected onto the stabilized model without contributing to calibration. Most of these samples occupied intermediate positions along the acoustic stress-response axis, indicating a graded metabolic response (Fig. 2A).

A second OPLS-DA model was applied to D-larvae exposed to chemical pollution (Fig. 2B; Table S3). This model, also comprising one predictive and one orthogonal component, showed high explanatory and predictive performance ($R^2Y = 0.99$, $Q^2 = 0.98$) and was statistically significant according to CV-ANOVA ($p = 5.89 \times 10^{-5}$). Fourteen annotated metabolites contributed to this axis (Fig. 2C).

The comparison of metabolite contributions indicated that four amino acids and trigonelline were involved in both acoustic and chemical stress responses in D-larvae, contributing in a similar direction on each stress-response axis (Fig. 2C).

3.2. Stage-specific modulation of metabolic responses in post-larvae

We then investigated the metabolic response of *M. edulis* post-larvae to vessel noise, embryonic chemical exposure, and sequential exposure involving embryonic chemical stress followed by acoustic exposure during metamorphosis by ^{1}H NMR. Our metabolomics analysis revealed marked differences in the metabolic responses of post-larvae exposed to acoustic stress, embryonic chemical exposure, or their combination. An OPLS-DA model contrasting ambient ($n = 10$) and high noise-exposed ($n = 9$) post-larvae was first adjusted (Fig. 3A; Table S4). This model, comprising one predictive and three orthogonal components, showed strong explanatory power and robustness ($R^2Y = 0.98$, $Q^2 = 0.90$) and was statistically significant according to CV-ANOVA ($p = 7.97 \times 10^{-5}$). The model defined an acoustic stress-response axis involving 17 annotated metabolites.

In the acoustics models, post-larval pools subjected to low and medium noise levels were projected onto the stabilized stress-response axis, where they occupied intermediate positions between the control and high-noise treatments, consistent with a dose-dependent metabolic response (Fig. 3A, C).

A second OPLS-DA model was applied to post-larvae originating from chemically exposed embryos ($n = 6$) (Fig. 3B; Table S5). This model included one predictive and two orthogonal components and showed a robust fit ($R^2Y = 0.99$, $Q^2 = 0.97$). The model was statistically significant according to CV-ANOVA ($p = 8.46 \times 10^{-5}$) and defined a carry-over chemical stress-response axis involving 20 annotated metabolites.

To examine the metabolic consequences of sequential chemical and acoustic exposure, a third OPLS-DA model was constructed comparing control post-larvae (n = 6) with those exposed to both high-level noise and chemical pollution (n = 6) (Fig. 3C; Table S6). This model, composed of one predictive and two orthogonal components, showed strong explanatory and predictive power ($R^2Y = 0.99$, $Q^2 = 0.98$) and was statistically significant according to CV-ANOVA ($p = 2.25 \times 10^{-6}$). Eighteen annotated metabolites contributed to a sequential combined exposure response axis distinct from those associated with the single-stressor conditions.

Metabolite contributions underlying the different stress-response axes are summarized in the contribution heatmap (Fig. 3D). Several metabolites were involved in multiple stress conditions. Four metabolites (Glu, Ile/Leu, pyroGlu, and acetoacetate) contributed to both acoustic and chemical stress responses. Four additional metabolites (Thr, β-Ala, maltose, and acetylcholine) were shared between acoustic

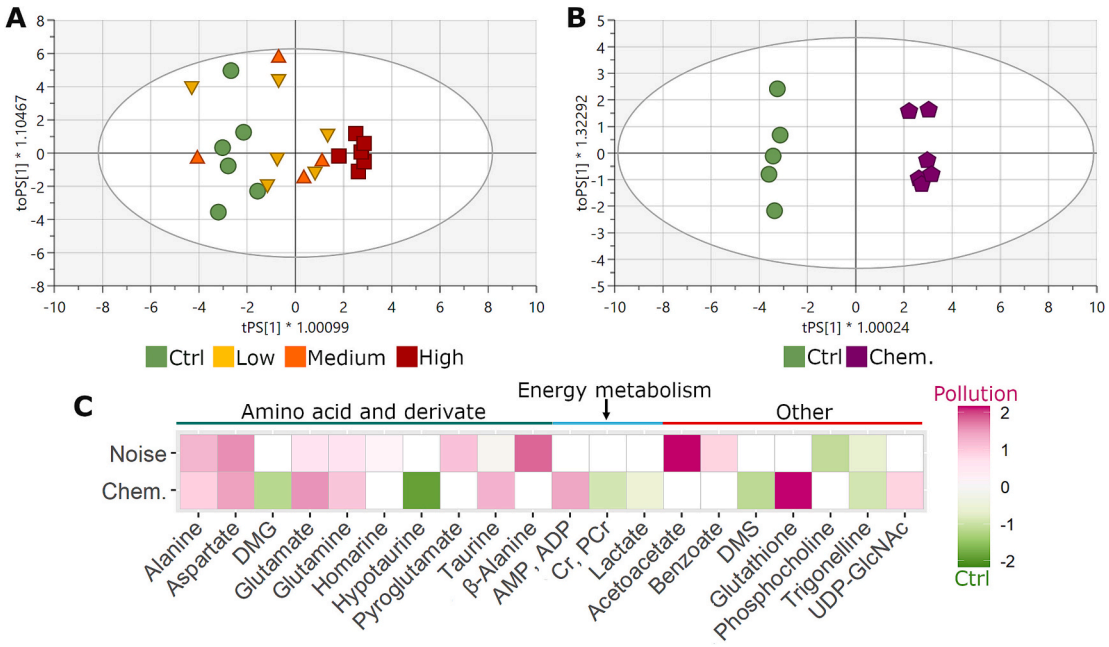

Fig. 2. Metabolomic responses of D-larvae to acoustic and chemical stressors by ^{1}H NMR. (A) OPLS-DA model contrasting control (green circle) and high (red box) acoustic exposure in D-larvae. Samples exposed to low (yellow inverted triangle) and medium (orange triangle) noise levels were projected onto the model without contributing to calibration, revealing a graded metabolomic response along the acoustic stress axis. (B) OPLS-DA model contrasting control and chemically (purple pentagon) exposed D-larvae. (C) Contribution heatmap showing metabolites contributing to the predictive components of the acoustic and chemical stress-response axes grouped by major metabolic pathways. DMG, dimethylglycine; Cr, creatine; PCr, phosphocreatine; DMS, dimethyl sulfone; UDP-GlcNAc, uridine diphosphate *N*-acetylglucosamine. (For interpretation of the references to colour in this figure legend, the reader is referred to the web version of this article.)

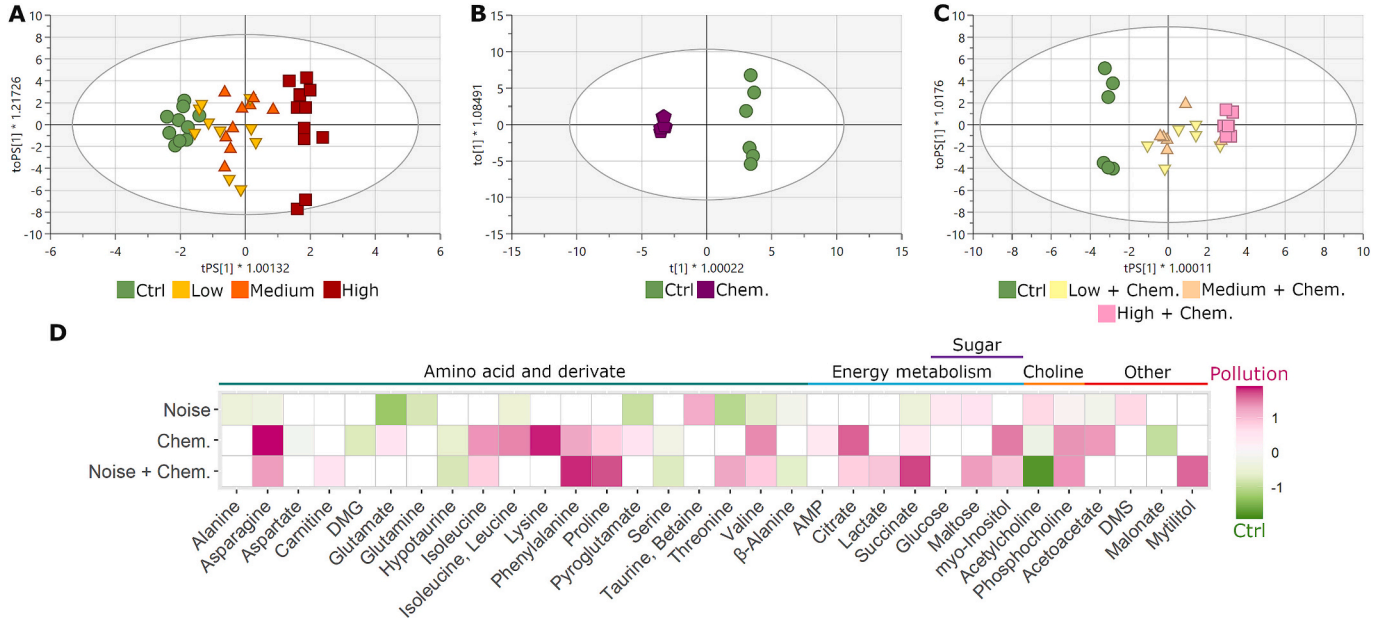

Fig. 3. Metabolomic responses of post-larvae to acoustic, chemical, and sequentially combined stressors. (A) OPLS-DA model contrasting control (green circle) and high (red box) acoustic exposure in post-larvae. Samples exposed to low (yellow inverted triangle) and medium (orange triangle) noise levels were projected onto the model without contributing to calibration. (B) OPLS-DA model contrasting control and chemically (purple pentagon) exposed post-larvae. (C) OPLS-DA model separating control and post-larvae sequentially exposed to chemical during embryogenesis and acoustic stress during metamorphosis (pink box) from controls. The intermediate noise levels were projected onto the model without contributing to calibration. (D) Contribution heatmap showing metabolites contributing to the predictive components of the acoustic, chemical, and combined stress-response axes, grouped by major metabolic pathways. DMG, dimethylglycine; DMS, dimethyl sulfone. (For interpretation of the references to colour in this figure legend, the reader is referred to the web version of this article.)

stress and the sequential combined acoustic-chemical condition, while seven metabolites (hypotaurine, Ile, Phe, Pro, Ser, citrate, and myo-inositol) were implicated in both chemical and sequential combined stress responses. Four metabolites (Asp, Val, succinate, and phosphocholine) contributed consistently across all three stress-response axes. For metabolites shared between chemical and sequential combined stress conditions, contributions were oriented in similar directions along the respective predictive components.

3.3. Metabolic pathway enrichment along stress-response axes

3.3.1. Pathway enrichment highlights shared core processes across stressors, with stage-specific emphasis

Pathway enrichment analysis was performed using metabolites contributing to the predictive components of the OPLS-DA models to identify metabolic processes associated with acoustic stress, chemical pollution, and sequential combined exposure (Fig. 4). In D-larvae, both acoustic and chemical stressors were associated with enrichment of pathways related to amino acid metabolism and nitrogen handling, including glutamate metabolism, glycine and serine metabolism, arginine and proline metabolism, ammonia recycling, and the urea cycle (Fig. 4A). Several pathways linked to central carbon metabolism, such as the malate–aspartate shuttle, pyruvate metabolism, and the glucose–alanine cycle, were also enriched under both stressors. While many pathways were shared between noise and chemical exposure, differences in enrichment magnitude and statistical significance were observed, indicating partially overlapping but non-identical metabolic responses.

In post-larvae, enrichment patterns differed from those observed in D-larvae (Fig. 4B). Pathways related to branched-chain amino acid degradation (valine, leucine, and isoleucine degradation), energy metabolism (ketone body metabolism, propanoate metabolism, Warburg effect), and mitochondrial shuttling (malate–aspartate shuttle) were enriched. Additional enrichment was observed for glutathione metabolism, ammonia recycling, and arginine and proline metabolism across stress conditions. Compared to D-larvae, post-larvae exhibited a stronger representation of pathways associated with energy metabolism.

3.3.2. Contribution-based grouping indicates overlapping between chemical and sequential combined stress responses

Comparison of metabolites contributing to the predictive components of the OPLS-DA models showed differential overlap between stress conditions and developmental stages. In D-larvae, some metabolites were shared between acoustic and chemical exposure, with several contributing similarly to both stress axes (Fig. 2C). These shared metabolites primarily belonged to amino acid metabolism and nitrogen-related pathways.

In post-larvae, the sequential combined noise and chemical exposure shared a larger number of contributing metabolites with the chemical-only treatment than with the noise-only treatment (Fig. 3D). Metabolites common to chemical and sequential combined stress conditions contributed in similar directions along the respective predictive components, whereas overlap with the noise-only model was more limited. This pattern indicates convergence of the response to sequential exposure toward the metabolic profile associated with chemical pollution.

4. Discussion

4.1. Environmental relevance and biological context of the stressors

The acoustic stressor used in this study corresponds to playbacks of one of the loudest commercial vessels recorded in the Saint-Pierre-et-Miquelon archipelago and is representative of shipping noise generated by large cargo ships (McKenna et al., 2012; Veillard et al., 2025a). While previous analyses showed that shipping noise exposure did not impair embryogenesis success (Veillard et al., 2025b), it moderately affected post-larval performance, with increased metamorphosis success under high noise exposure and small but significant differences in size at metamorphosis (Veillard et al., 2025a). As bivalves lack auditory organs, responses are most likely mediated by sensitivity to particle motion and substrate-borne vibration rather than "hearing" per se.

Chemical exposure involved a contaminant cocktail representative of pollution associated with industrial ports and maritime traffic, including dissolved copper, lead, mercury, and petroleum-derived hydrocarbons (Veillard et al., 2026). Chemical accumulation analyses confirmed effective internal exposure, with elevated concentrations of Cu^{2+}, Pb^{2+}, and alkanes in D-larvae and persistent accumulation of lead throughout post-larval development. Although chemical exposure did not significantly affect embryogenesis success or early larval size, post-metamorphic size and growth were increased (Veillard, 2025; Veillard et al., 2026). This pattern may reflect selective pressure during embryonic development, whereby more sensitive individuals were eliminated, resulting in a population of surviving larvae with enhanced growth performance. To facilitate integration of the metabolomic responses with previously reported developmental and physiological observations, the main phenotypic effects associated with each exposure condition are summarized in Table 1.

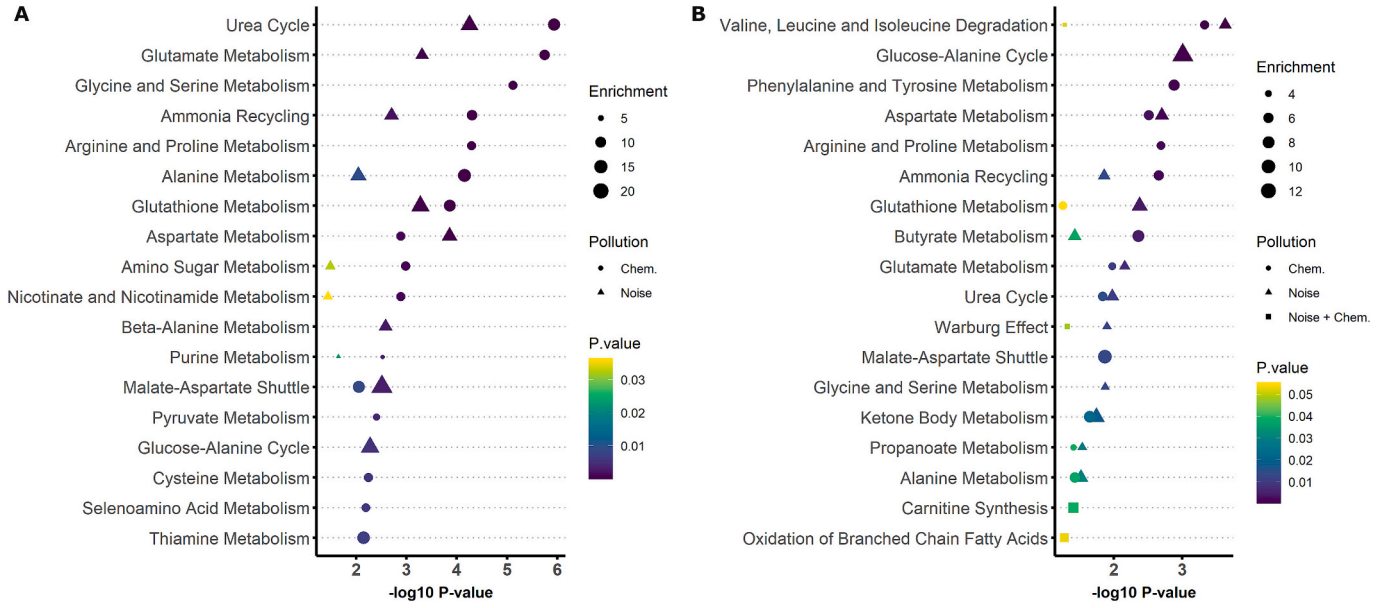

Fig. 4. Functional enrichment of metabolites contributing to stress-response axes. Pathway enrichment analysis of metabolites contributing to the predictive components of OPLS-DA stress-response axes in (A) D-larvae, and (B) post-larvae. Enrichment results are shown for acoustic stress, chemical pollution, and sequential combined exposure. Pathways are ordered by significance ($-\log_{10}$ *P*-value) with symbol size indicating their enrichment.

Table 1
Summary of the main physiological and developmental responses previously reported in blue mussel larvae exposed to shipping-related acoustic and chemical stressors across developmental stages.

Developmental stage	Exposure condition	Physiological / developmental response	Observations[a]	Source
D-larvae	Shipping noise	Embryogenesis success	No significant effect	Veillard et al., 2025b
		D-larval size	No significant effect	
	Chemical contamination (early July spawning event)	Embryogenesis success	No significant effect	Veillard et al., 2026
		D-larval size	No significant effect	
Post-larvae	Shipping noise	Metamorphosis success	+21% (High vs. Ctrl)	Veillard et al., 2025a
		Size at metamorphosis (PII)	+8.8% (Low vs. Ctrl) − 6.5% (High vs. Low)	
		Post-metamorphosis growth (D)	+78% trend (High vs. Ctrl; $P = 0.1$)	
		Delayed metamorphosis	Settlement delayed until ~300 μm	
	Embryonic chemical exposure (carry-over)	Metamorphosis success	No significant effect	Veillard, 2025
		Size at metamorphosis (PII)	+23% (Carry-over vs. Ctrl)	
		Post-metamorphosis growth (D)	+76% (Carry-over vs. Ctrl)	
	Embryonic chemical exposure (carry-over) + noise	Metamorphosis success	No significant effect	
		Size at metamorphosis (PII)	No significant effect	
		Post-metamorphosis growth (D)	+118% (High vs. Ctrl) + 101% (High vs. Low)	

[a] Percentages indicate relative differences between treatment means. Only statistically significant differences are shown unless otherwise specified.

In this context, metabolomic analyses can reveal biochemical adjustments that may precede, or occur in the absence of, detectable phenotypic effects. The following sections therefore explore how metabolic responses vary across developmental stages and between stressor types.

4.2. Stage-specific metabolic sensitivity to shipping-related stressors

Across both shipping noise playbacks and chemical exposures, D-larvae and post-larvae of *Mytilus edulis* displayed distinct metabolic sensitivities to shipping-related stressors, consistent with differences in physiological organization between embryonic and post-metamorphic stages. These differences were reflected in the number and functional categories of metabolites contributing to stress-response axes.

In D-larvae, metabolic responses were characterized by changes in a relatively limited set of metabolites, dominated by amino acids and their derivatives. Amino acids play crucial roles in protein synthesis, energy metabolism, and osmotic regulation (Cappello et al., 2018). D-larvae development are supported by maternally provisioned reserves to sustain protein synthesis and energy production, with a limited capacity for metabolic compensation (Sánchez-Lazo and Martínez-Pita, 2012). As a result, the modulation of free amino acid pools represents one of the primary adjustable components of larval metabolism at this stage. Accordingly, metabolites contributing to stress-response axes were largely associated with free and protein-derived amino acid metabolism and nitrogen handling, including alanine, aspartate, glutamate, glutamine, β-alanine, and related compounds. Because external nutrient uptake is negligible at this stage (Lucas et al., 1986), shifts in soluble metabolite pools primarily reflect redistribution among endogenous reserves rather than changes in substrate supply. Shifts in the relative contribution of these metabolites are therefore consistent with altered protein turnover and redistribution of free amino-acid pools under stress, suggesting constrained physiological options during early development (Pytharopoulou et al., 2006; Veillard et al., 2026, 2025a, 2025b; Viarengo et al., 1982).

In post-larvae, stress-related metabolic reactions involved a larger number of metabolites and covered a broader range of metabolic functions. These metabolites included amino acids, intermediates of central carbon metabolism such as citrate, succinate, acetoacetate, and lactate, as well as compounds associated with carbohydrate metabolism (e.g., maltose, glucose), membrane-related processes (e.g., phosphocholine, myo-inositol), and redox-associated pathways (e.g., hypotaurine). This broader metabolic engagement reflects the transition to exogenous feeding, increased tissue differentiation, and higher energetic demands associated with settlement and post-metamorphic growth. Unlike D-larvae, post-larvae can modulate both substrate acquisition and intracellular metabolic fluxes, enabling greater metabolic plasticity in response to environmental stress. This capacity allows metabolic reorganization to occur across multiple interconnected pathways rather than being restricted to redistribution of internal amino acid pools. Such flexibility is consistent with the onset of feeding, activation of digestive processes, and expansion of mitochondrial oxidative metabolism following metamorphosis (May et al., 2017; Noisette et al., 2021).

Taken together, our results indicate that developmental stage strongly determines both the scope and nature of metabolic responses to environmental stressors. Embryonic stages exhibit constrained responses largely centred on amino acid metabolism and nitrogen handling, whereas post-larvae display more extensive metabolic reorganization involving central energy and membrane-associated pathways. This developmental shift provides the physiological basis for the stressor-specific metabolic strategies observed during growth and metamorphosis, including the altered metamorphosis success, post-metamorphic growth, and size-related responses summarized in Table 1, which are examined in greater detail in Section 4.3.

4.3. Developmental modulation of stressor-specific metabolic responses

4.3.1. Embryogenesis: similar metabolic responses to shipping noise and chemical stress

During embryogenesis, metabolic responses to shipping noise and chemical stressors were largely overlapping. Amino acids and their derivatives were the most discriminant metabolites under both exposures in the D-larvae, indicating that stress responses primarily involved modulation of protein turnover and nitrogen-associated pathway. Several amino acids (Asp, Glu, Gln, pyroGlu, Ala) were elevated under both stressors, consistent with altered protein turnover and redistribution of free amino acid pools. In mussels, such responses are commonly associated with metabolic depression and maintenance of cellular homeostasis under stressful conditions, including exposure to heavy metals or xenobiotics (Pytharopoulou et al., 2006; Viarengo et al., 1982). Given the endotrophic nature of this developmental stage (Lucas et al., 1986), such modulation likely reflects limited physiological options, with protein pools serving both biosynthetic and energetic roles.

Limited divergence between stressors was observed in energy-related metabolites. Shipping noise exposure was associated with increased acetoacetate, suggesting mobilisation of lipid reserves via β-oxidation and use of alternative energy substrates when carbohydrate availability is limited. Similar responses have been reported in mussels from petrochemical areas and interpreted as compensatory mobilisation of energy reserves under unfavourable conditions (Cappello et al., 2013b).

In contrast, chemical exposure resulted in decreased creatine/phosphocreatine and lactate, together with increased ATP hydrolysis products, indicating reduced capacity for ATP regeneration and faster depletion of energy reserves (Smolders et al., 2004).

Osmolyte-related metabolites also showed stressor-dependent modulation. In mussels, free amino acid pools play a role in osmotic regulation, with aminopeptidase I contributing to protein degradation to maintain cellular isoconformity (Hilbish and Koehn, 1987). Here, alanine, homarine, and β-alanine were elevated under shipping noise exposure, whereas alanine and taurine were elevated under chemical exposure, indicating stressor-specific modulation of osmolyte balance.

In addition, antioxidant thio-metabolites such as glutathione and dimethyl sulfone were specifically regulated under chemical exposure, consistent with activation of redox and detoxification pathways associated with metal and hydrocarbon stress. Indeed, glutathione is a key cellular antioxidant and metal detoxification molecule, often regulated in response to heavy metals and xenobiotics as part of oxidative stress defence systems in aquatic organisms (Canesi et al., 1999), and related organosulfur compounds such as dimethyl sulfone and taurine have been implicated in modulation of oxidative stress in biological systems (Butawan et al., 2017; Oliveira et al., 2010).

Despite these mechanistic differences, most discriminant metabolites were shared between stressors and varied in similar directions, indicating that embryonic metabolism responds to different environmental pressures through largely similar biochemical strategies. Embryogenesis success and D-larval size remained nevertheless unaffected under the exposure conditions tested (Table 1), suggesting that these metabolic adjustments may represent compensatory responses maintaining early developmental performance.

4.3.2. *Metamorphosis: contrasted metabolic responses to acoustic and chemical stress*

At the post-larval stage, contribution-based analyses revealed stronger contrast between metabolic responses to shipping noise and chemical stress than observed during embryogenesis. Although a small subset of metabolites contributed to both stress-response axes, and most did so in opposite direction on the stress-response axis, the majority of discriminant metabolites were stressor-specific, indicating distinct physiological constraints operating during metamorphosis.

Under shipping noise exposure, metabolites contributing to the stress-response axis included amino acids, intermediates of central carbon metabolism (succinate, maltose, glucose), the ketone body acetoacetate, and the neurotransmitter acetylcholine. Amino acids, succinate, and acetoacetate contributed in the same direction (Fig. 3D) and were relatively lower within the pool of soluble metabolites, consistent with increased utilization of these substrates to sustain mitochondrial energy production during metamorphosis (Moyes et al., 1990; Veillard et al., 2025a). In contrast, maltose and glucose were relatively higher under shipping noise exposure, suggesting compensatory mobilisation of carbohydrate reserves to support energy-intensive processes associated with settlement and tissue differentiation. These metabolic changes are consistent with the increased metamorphosis success, delayed settlement, and growth-related responses previously observed under shipping-noise exposure (Table 1). The contribution of acetylcholine further supports modulation of settlement-related processes (Beiras and Widdows, 1995). Additional contributions from β-alanine, taurine, betaine, and dimethyl sulfone indicate adjustments in osmotic and redox balances accompanying tissue reorganization and post-metamorphic development.

Under chemical exposure, post-larval metabolic profiles contrasted with those observed under shipping noise stress. Amino acids, tricarboxylic acid cycle intermediates, and acetoacetate contributed in the opposite direction (Fig. 3D) and were relatively higher within the pool of soluble metabolites in post-larvae originating from chemically exposed embryos, indicating reduced utilization and accumulation of metabolic intermediates. The positive contribution of adenosine monophosphate (AMP) suggests impaired ATP regeneration and lower cellular energy charge, consistent with altered mitochondrial energy metabolism and impaired oxidative phosphorylation commonly reported under metal stress (Wu and Wang, 2010). Because chemical exposure occurred only during embryogenesis and was absent during metamorphosis, these patterns indicate persistent metabolic constraints rather than direct toxic effects during metamorphosis.

The accumulation of free amino acids is consistent with altered protein and nitrogen metabolisms commonly reported in contaminant-exposed bivalves (Pytharopoulou et al., 2006; Viarengo et al., 1982). In addition, the inverse contribution of acetylcholine relative to shipping noise exposure suggests disruption of neuromodulatory processes involved in settlement. Contributions from phosphocholine and myo-inositol further indicate perturbation of membrane integrity and lysosomal stability under chemical stress (Viarengo et al., 2007).

Overall, our results indicate that playbacks of shipping noise are associated with increased metabolic turnover in post-larvae, reflecting higher energetic demands during metamorphosis, whereas embryonic chemical exposure leads to persistent alterations in the energy metabolism that limit substrate utilization and cellular maintenance.

To synthesize these stage- and stressor-specific metabolic patterns, Fig. 5 summarizes the dominant metabolic trajectories observed during embryogenesis and metamorphosis under acoustic, chemical, and sequential combined exposures.

4.4. *Sequential combined exposure reveals dominance of chemical carry-over effects*

At the post-larval stage, sequential exposure involving embryonic chemical stress followed by acoustic exposure during metamorphosis produced a metabolic profile that more closely resembled the carry-over chemical stress-response axis than the acoustic one. Most metabolites contributing to the sequential combined stress-response axis were shared with the chemical-only condition and varied in the same direction, whereas overlap with the shipping noise-only response was limited (Fig. 3D). This pattern suggests a predominance of carry-over effects from chemical-induced metabolic constraints under sequential combined exposure. Such non-additive responses, where one stressor dominates the integrated physiological outcome, are commonly reported in multi-stressor studies when prior or stronger stressors constrain subsequent adaptive capacity (Crain et al., 2008; Rynkowski et al., 2025). This is further supported by experimental studies in mussels showing that prior exposure to environmental stressors can lead to lasting physiological constraints that limit the response to subsequent stressors, even if they differ in nature (Chapuis et al., 2025).

Shared metabolites between chemical and sequential combined exposure included several amino acids (Asn, Ile, Phe, Pro, Ser, Val), central carbon metabolism intermediates (citrate, succinate), membrane-related metabolites (phosphocholine, myo-inositol), and redox- or osmolyte-associated compounds (hypotaurine). These metabolites showed a similar contribution under chemical and sequential combined exposures, indicating persistent constraints on protein metabolism, mitochondrial function, and membrane homeostasis in post-larvae originating from chemically exposed embryos.

In contrast, metabolites characteristic of the acoustic stress response, including carbohydrate-related metabolites and neuromodulatory compounds, showed weaker or inconsistent contributions to the sequential combined stress-response axis. Together, our results suggest that early chemical exposure limits metabolic flexibility during metamorphosis and reduces the expression of metabolic responses otherwise induced by shipping noise stress. Although both chemical and acoustic stressors were associated with enhanced post-metamorphic growth (Table 1), the metabolomic response to sequential exposure remained predominantly structured by metabolites characteristic of the chemical carry-over response. This indicates that similar developmental outcomes may arise from distinct underlying metabolic trajectories and highlights

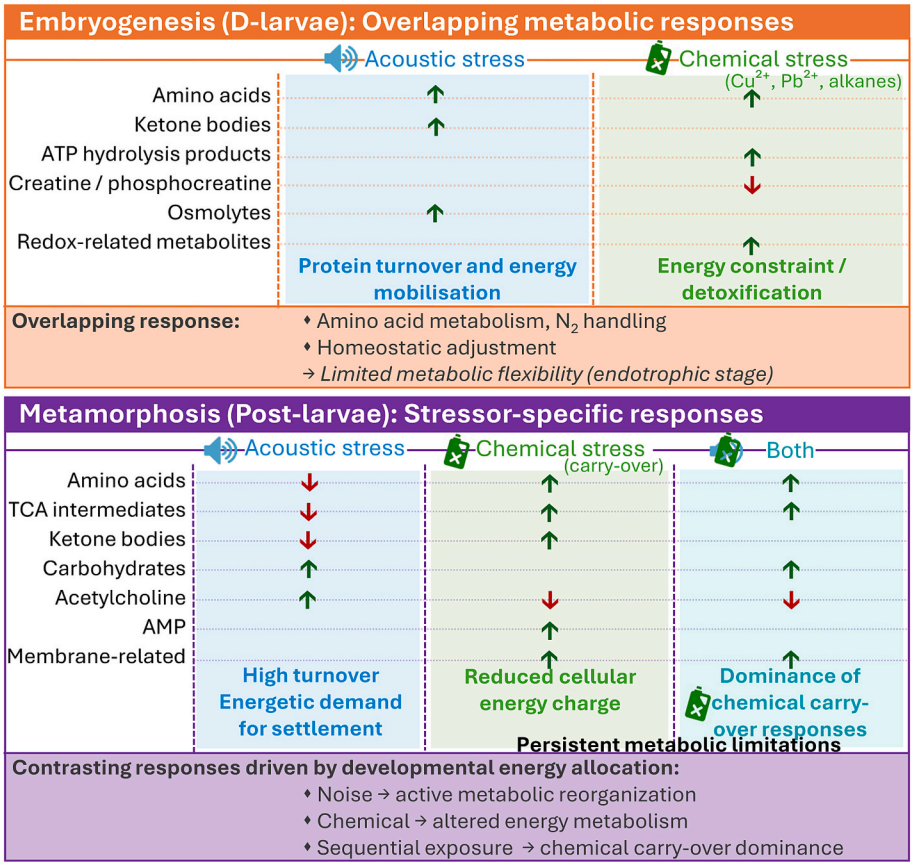

Fig. 5. Summary of stage-specific metabolic responses to acoustic, chemical, and combined stressors in *Mytilus edulis* early life stages. Synthesis of similar metabolic responses during embryogenesis and stressor-specific metabolic trajectories during metamorphosis, highlighting chemical-driven dominance under sequential combined exposure. Arrows indicate the direction of metabolite contribution along the stress-response axes relative to control conditions. TCA, tricarboxylic acid cycle.

the persistence of chemical-induced physiological constraints across developmental stages.

5. Conclusion

Shipping-related acoustic and chemical stressors affect mussel metabolism in a stage-dependent manner. Embryonic responses were largely overlapping and dominated by amino acid metabolism, whereas metamorphosis exhibited stressor-specific metabolic strategies, with shipping noise exposure promoting increased energetic turnover whereas embryonic chemical exposure induced persistent metabolic constraints that remained detectable during later metamorphosis.

The graded positioning of larval pools along acoustic stress-response axes at intermediate noise levels indicates that metabolic responses to shipping noise follow a progressive dose–response pattern. This suggests the existence of biologically-relevant exposure thresholds consistent with recent efforts to define operational noise benchmarks for environmental management in European waters (El-Dairi et al., 2026).

By constraining energy balance and cellular homeostasis during critical developmental windows, early-life exposure to shipping-related stressors may influence key physiological processes associated with growth, settlement, and survival as reflected by the developmental responses summarized in Table 1. Such persistent metabolic effects could contribute to performance variability in chronically exposed environments and may help explain the differentiation observed between harbor-associated and natural mussel populations (Simon et al., 2020).

Overall, these findings indicate that chronic maritime pollution can shape early physiological trajectories, with potential long-term ecological and evolutionary consequences.

CRediT authorship contribution statement

Stéphane Beauclercq: Writing – review & editing, Writing – original draft, Visualization, Methodology, Investigation, Formal analysis, Data curation, Conceptualization. **Delphine Veillard:** Writing – review & editing, Methodology, Investigation, Conceptualization. **Richard Saint-Louis:** Writing – review & editing, Methodology, Conceptualization. **Frédéric Olivier:** Writing – review & editing, Project administration, Funding acquisition, Conceptualization. **Dror E. Warschawski:** Writing – review & editing, Conceptualization. **Réjean Tremblay:** Writing – review & editing, Project administration, Funding acquisition, Conceptualization. **Isabelle Marcotte:** Writing – review & editing, Project administration, Funding acquisition, Conceptualization.

Funding

This study was funded by the Fonds de la Recherche du Quebec Nature et Technologies (FRQNT, 280057) and the Agence Nationale de la Recherche (ANR-19-FQSM-0005) through the French-Quebec maritime funding program. Supplementary funds were also obtained from the Ressources Aquatiques Quebec Research Network (FRQNT, #2014-RS-171172). This study is a contribution to the BeBEST2 International Research Project (CNRS INEE/LEMAR and UQAR/ISMER).

Declaration of competing interest

The authors declare that they have no known competing financial interests or personal relationships that could have influence the work reported in this paper.

Acknowledgements

We thank Lindsay Peyriga for her help in setting up the NMR experiments on the Bruker Ascend 800 MHz spectrometer equipped with a 1.7 mm cryoprobes from the MetaboHUB-MetaToul facility (ANR-11-INBS-0010). We acknowledge access, for method development purposes, to the biomolecular NMR platform of the Institut de biologie physico-chimique (IBPC) supported by the CNRS, the Labex DYNAMO (ANR-11-LABX-0011), the Equipex CACSICE (ANR-11-EQPX-0008), and the Conseil Régional d'Île-de-France (SESAME grant). The authors thank Alexandre A. Arnold for helpful comments on the manuscript.

The authors acknowledge the use of ChatGPT (OpenAI) as a language-support tool to improve the clarity and organization of the manuscript text. All scientific content, data analysis, interpretation, and conclusions were generated and verified by the authors.

Appendix A. Supplementary data

The supplementary material includes representative annotated ^{1}H NMR spectra and tables listing the replication design, and the chemical shifts and metabolite assignments of the spectral buckets retained in the OPLS-DA models.

Data availability

The NMR-based metabolomic datasets generated from D-larvae (experiments 1 and 3) and post-larvae (experiments 2 and 3) analysed in the present study are available in the MetaboLights repository (EMBL-EBI) (Haug et al., 2020) under accession number MTBLS13945. The NMR-based metabolomic dataset generated from post-larvae of experiment 1 has been previously deposited under accession number MTBLS5678.

References

Aru, V., Motawie, M.S., Khakimov, B., Sørensen, K.M., Møller, B.L., Engelsen, S.B., 2020. First-principles identification of C-methyl-scyllo-inositol (mytilitol) - a new species-specific metabolite indicator of geographic origin for marine bivalve molluscs (*Mytilus* and *Ruditapes spp*). Food Chem. 328, 126959. https://doi.org/10.1016/j.foodchem.2020.126959.

Beauclercq, S., Mignon-Grasteau, S., Petit, A., Berger, Q., Lefèvre, A., Métayer-Coustard, S., Tesseraud, S., Emond, P., Berri, C., Le Bihan-Duval, E., 2022. A divergent selection on breast meat ultimate pH, a key factor for chicken meat quality, is associated with different circulating lipid profiles. Front. Physiol. 13. https://doi.org/10.3389/fphys.2022.935868.

Beiras, R., Widdows, J., 1995. Induction of metamorphosis in larvae of the oyster Crassostrea gigas using neuroactive compounds. Mar. Biol. 123, 327–334. https://doi.org/10.1007/BF00353624.

Blom, E.-L., Kvarnemo, C., Dekhla, I., Schöld, S., Andersson, M.H., Svensson, O., Amorim, M.C.P., 2019. Continuous but not intermittent noise has a negative impact on mating success in a marine fish with paternal care. Sci. Rep. 9, 5494. https://doi.org/10.1038/s41598-019-41786-x.

Breitwieser, M., Viricel, A., Graber, M., Murillo, L., Becquet, V., Churlaud, C., Fruitier-Arnaudin, I., Huet, V., Lacroix, C., Pante, E., Floch, S.L., Thomas-Guyon, H., 2016. Short-term and long-term biological effects of chronic chemical contamination on natural populations of a marine bivalve. PLoS One 11, e0150184. https://doi.org/10.1371/journal.pone.0150184.

Butawan, M., Benjamin, R.L., Bloomer, R.J., 2017. Methylsulfonylmethane: applications and safety of a novel dietary supplement. Nutrients 9, 290. https://doi.org/10.3390/nu9030290.

Byrnes, T.A., Dunn, R.J.K., Byrnes, T.A., Dunn, R.J.K., 2020. Boating- and shipping-related environmental impacts and example management measures: a review. J. Mar. Sci. Eng. 8. https://doi.org/10.3390/jmse8110908.

Calgaro, L., Cecchetto, M., Giubilato, E., Jalkanen, J.-P., Majamäki, E., Ytreberg, E., Hassellöv, I.-M., Fridell, E., Semenzin, E., Marcomini, A., 2025. The contribution of shipping to the emission of water and air pollutants in the northern Adriatic Sea - current and future scenarios. Mar. Pollut. Bull. 212, 117573. https://doi.org/10.1016/j.marpolbul.2025.117573.

Canesi, L., Viarengo, A., Leonzio, C., Filippelli, M., Gallo, G., 1999. Heavy metals and glutathione metabolism in mussel tissues. Aquat. Toxicol. 46, 67–76. https://doi.org/10.1016/S0166-445X(98)00116-7.

Cappello, T., Maisano, M., D'Agata, A., Natalotto, A., Mauceri, A., Fasulo, S., 2013a. Effects of environmental pollution in caged mussels (*Mytilus galloprovincialis*). Mar. Environ. Res. Next Gener. Ecotoxicol. 91, 52–60. https://doi.org/10.1016/j.marenvres.2012.12.010.

Cappello, T., Mauceri, A., Corsaro, C., Maisano, M., Parrino, V., Lo Paro, G., Messina, G., Fasulo, S., 2013b. Impact of environmental pollution on caged mussels *Mytilus galloprovincialis* using NMR-based metabolomics. Mar. Pollut. Bull. 77, 132–139. https://doi.org/10.1016/j.marpolbul.2013.10.019.

Cappello, T., Giannetto, A., Parrino, V., Maisano, M., Oliva, S., De Marco, G., Guerriero, G., Mauceri, A., Fasulo, S., 2018. Baseline levels of metabolites in different tissues of mussel *Mytilus galloprovincialis* (Bivalvia: Mytilidae). Compar. Biochem. Physiol. Part D: Genom. Proteom. 26, 32–39. https://doi.org/10.1016/j.cbd.2018.03.005.

Chapuis, A.F., Wale, M.A., Bailey, M., Farley, H.M., Bean, T.P., Regan, T., 2025. Anthropogenic noise exposure suppresses the immune response in *Mytilus* spp. following *Vibrio splendidus* challenge. Front. Immunol. 16. https://doi.org/10.3389/fimmu.2025.1657667.

Chauvaud, S., Chauvaud, L., Jolivet, A., 2018. Impacts Des Sons Anthropiques Sur la Faune Marine. Éditions Quae, Paris.

Crain, C.M., Kroeker, K., Halpern, B.S., 2008. Interactive and cumulative effects of multiple human stressors in marine systems. Ecol. Lett. 11, 1304–1315. https://doi.org/10.1111/j.1461-0248.2008.01253.x.

Duarte, C.M., Chapuis, L., Collin, S.P., Costa, D.P., Devassy, R.P., Eguiluz, V.M., Erbe, C., Gordon, T.A.C., Halpern, B.S., Harding, H.R., Havlik, M.N., Meekan, M., Merchant, N.D., Miksis-Olds, J.L., Parsons, M., Predragovic, M., Radford, A.N., Radford, C.A., Simpson, S.D., Slabbekoorn, H., Staaterman, E., Van Opzeeland, I.C., Winderen, J., Zhang, X., Juanes, F., 2021. The soundscape of the Anthropocene ocean. Science 371, eaba4658. https://doi.org/10.1126/science.aba4658.

El-Dairi, R., Pöyhönen, V., Turja, R., Outinen, O., Lehtonen, K.K., 2026. Behavioural and biochemical effects of underwater noise from vessel traffic on Baltic sea mussels (*Mytilus* spp.). Mar. Environ. Res. 216, 107870. https://doi.org/10.1016/j.marenvres.2026.107870.

Erbe, C., Marley, S.A., Schoeman, R.P., Smith, J.N., Trigg, L.E., Embling, C.B., 2019. The effects of ship noise on marine mammals: a review. Front. Mar. Sci. 6. https://doi.org/10.3389/fmars.2019.00606.

Eriksson, L., Trygg, J., Wold, S., 2008. CV-ANOVA for significance testing of PLS and OPLS models. J. Chemom. 22, 594–600. https://doi.org/10.1002/cem.1187.

Folch, J., Lees, M., Sloane Stanley, G.H., 1957. A simple method for the isolation and purification of total lipides from animal tissues. J. Biol. Chem. 226, 497–509.

Frizzo, R., Bortoletto, E., Riello, T., Leanza, L., Schievano, E., Venier, P., Mammi, S., 2021. NMR metabolite profiles of the bivalve mollusc *Mytilus galloprovincialis*before and after immune stimulation with *Vibrio splendidus*. Front. Mol. Biosci. 8, 731. https://doi.org/10.3389/FMOLB.2021.686770/BIBTEX.

Halpern, B.S., Frazier, M., Potapenko, J., Casey, K.S., Koenig, K., Longo, C., Lowndes, J. S., Rockwood, R.C., Selig, E.R., Selkoe, K.A., Walbridge, S., 2015. Spatial and temporal changes in cumulative human impacts on the world's ocean. Nat. Commun. 6, 7615. https://doi.org/10.1038/ncomms8615.

Haug, K., Cochrane, K., Nainala, V.C., Williams, M., Chang, J., Jayaseelan, K.V., O'Donovan, C., 2020. MetaboLights: a resource evolving in response to the needs of its scientific community. Nucleic Acids Res. 48, D440–D444. https://doi.org/10.1093/nar/gkz1019.

Hilbish, T.J., Koehn, R.K., 1987. The adaptive importance of genetic variation. Am. Sci. 75, 134–141.

Hubert, J., Booms, E., Witbaard, R., Slabbekoorn, H., 2022. Responsiveness and habituation to repeated sound exposures and pulse trains in blue mussels. J. Exp. Mar. Biol. Ecol. 547, 151668. https://doi.org/10.1016/j.jembe.2021.151668.

Jacob, D., Deborde, C., Lefebvre, M., Maucourt, M., Moing, A., 2017. NMRProcFlow: a graphical and interactive tool dedicated to 1D spectra processing for NMR-based metabolomics. Metabolomics 13, 36. https://doi.org/10.1007/s11306-017-1178-y.

Jalkanen, J.-P., Johansson, L., Andersson, M.H., Majamäki, E., Sigray, P., 2022. Underwater noise emissions from ships during 2014–2020. Environ. Pollut. 311, 119766. https://doi.org/10.1016/j.envpol.2022.119766.

Jolivet, A., Tremblay, R., Olivier, F., Gervaise, C., Sonier, R., Genard, B., Chauvaud, L., 2016. Validation of trophic and anthropic underwater noise as settlement trigger in blue mussels. Sci. Rep. 6, 33829. https://doi.org/10.1038/srep33829.

Kotta, J., Futter, M., Kaasik, A., Liversage, K., Rätsep, M., Barboza, F.R., Bergström, L., Bergström, P., Bobsien, I., Díaz, E., Herkül, K., Jonsson, P.R., Korpinen, S., Kraufvelin, P., Krost, P., Lindahl, O., Lindegarth, M., Lyngsgaard, M.M., Mühl, M., Sandman, A.N., Orav-Kotta, H., Orlova, M., Skov, H., Rissanen, J., Šiaulys, A., Vidakovic, A., Virtanen, E., 2020. Cleaning up seas using blue growth initiatives: mussel farming for eutrophication control in the Baltic Sea. Sci. Total Environ. 709, 136144. https://doi.org/10.1016/j.scitotenv.2019.136144.

Lehtonen, K.K., Leiniö, S., Schneider, R., Leivuori, M., 2006. Biomarkers of pollution effects in the bivalves *Mytilus edulis* and *Macoma balthica* collected from the southern coast of Finland (Baltic Sea). Mar. Ecol. Prog. Ser. 322, 155–168. https://doi.org/10.3354/meps322155.

Lillis, A., Eggleston, D.B., Bohnenstiehl, D.R., 2016. Soundscapes and larval settlement: Characterizing the stimulus from a larval perspective. In: Popper, A.N., Hawkins, A. (Eds.), The Effects of Noise on Aquatic Life II, Advances in Experimental Medicine and Biology. Springer, New York, NY, pp. 637–645. https://doi.org/10.1007/978-1-4939-2981-8_77.

Lucas, A., Chebab-Chalabi, L., Aldana Aranda, D., 1986. Passage de l'endotrophie à l'exotrophie chez les larves de *Mytilus edulis*. Oceanol. Acta 9.

Masud, N., Hayes, L., Crivelli, D., Grigg, S., Cable, J., 2020. Noise pollution: acute noise exposure increases susceptibility to disease and chronic exposure reduces host survival. R. Soc. Open Sci. 7, 200172. https://doi.org/10.1098/rsos.200172.

May, M.A., Bishop, K.D., Rawson, P.D., 2017. NMR profiling of metabolites in larval and juvenile blue mussels (Mytilus edulis) under ambient and low salinity conditions. Metabolites 7, 33. https://doi.org/10.3390/METABO7030033.

McDonald, M.A., Hildebrand, J.A., Wiggins, S.M., 2006. Increases in deep ocean ambient noise in the Northeast Pacific west of San Nicolas Island, California. J. Acoust. Soc. Am. 120, 711–718. https://doi.org/10.1121/1.2216565.

McKenna, M.F., Ross, D., Wiggins, S.M., Hildebrand, J.A., 2012. Underwater radiated noise from modern commercial ships. J. Acoust. Soc. Am. 131, 92–103. https://doi.org/10.1121/1.3664100.

Mearns, A.J., Reish, D.J., Oshida, P.S., Ginn, T., Rempel-Hester, M.A., Arthur, C., Rutherford, N., Pryor, R., 2015. Effects of pollution on marine organisms. Water Environ. Res. 87, 1718–1816. https://doi.org/10.2175/106143015X14338845156380.

Moyes, C.D., Suarez, R.K., Hochachka, P.W., Ballantyne, J.S., 1990. A comparison of fuel preferences of mitochondria from vertebrates and invertebrates. Can. J. Zool. 68, 1337–1349. https://doi.org/10.1139/z90-201.

Noisette, F., Calosi, P., Madeira, D., Chemel, M., Menu-Courey, K., Piedalue, S., Gurney-Smith, H., Daoud, D., Azetsu-Scott, K., 2021. Tolerant larvae and sensitive juveniles: integrating metabolomics and whole-organism responses to define life-stage specific sensitivity to ocean acidification in the American lobster. Metabolites 11, 584. https://doi.org/10.3390/metabo11090584.

Oliveira, M.W.S., Minotto, J.B., de Oliveira, M.R., Zanotto-Filho, A., Behr, G.A., Rocha, R. F., Moreira, J.C.F., Klamt, F., 2010. Scavenging and antioxidant potential of physiological taurine concentrations against different reactive oxygen/nitrogen species. Pharmacol. Rep. 62, 185–193. https://doi.org/10.1016/S1734-1140(10)70256-5.

Olivier, F., Gigot, M., Mathias, D., Jezequel, Y., Meziane, T., L'Her, C., Chauvaud, L., Bonnel, J., 2023. Assessing the impacts of anthropogenic sounds on early stages of benthic invertebrates: the "Larvosonic system". Limnol. Oceanogr. Methods 21, 53–68. https://doi.org/10.1002/LOM3.10527.

Pang, Z., Lu, Y., Zhou, G., Hui, F., Xu, L., Viau, C., Spigelman, A.F., MacDonald, P.E., Wishart, D.S., Li, S., Xia, J., 2024. MetaboAnalyst 6.0: towards a unified platform for metabolomics data processing, analysis and interpretation. Nucleic Acids Res. 52, W398–W406. https://doi.org/10.1093/nar/gkae253.

Popper, A.N., Hawkins, A.D., 2019. An overview of fish bioacoustics and the impacts of anthropogenic sounds on fishes. J. Fish Biol. 94, 692–713. https://doi.org/10.1111/jfb.13948.

Pytharopoulou, S., Kouvela, E.C., Sazakli, E., Leotsinidis, M., Kalpaxis, D.L., 2006. Evaluation of the global protein synthesis in *Mytilus galloprovincialis* in marine pollution monitoring: seasonal variability and correlations with other biomarkers. Aquat. Toxicol. 80, 33–41. https://doi.org/10.1016/j.aquatox.2006.07.010.

Rayssac, N., Pernet, F., Lacasse, O., Tremblay, R., 2010. Temperature effect on survival, growth, and triacylglycerol content during the early ontogeny of Mytilus edulis and M. trossulus. Mar. Ecol. Prog. Ser. 417, 183–191. https://doi.org/10.3354/meps08774.

Regoli, F., Giuliani, M.E., 2014. Oxidative pathways of chemical toxicity and oxidative stress biomarkers in marine organisms. Mar. Environ. Res. 93, 106–117. https://doi.org/10.1016/j.marenvres.2013.07.006.

Richardson . Jr, C.R.G., W.J., Malme, C.I., Thomson, D.H., 2013. Marine Mammals and Noise. Academic Press.

Rynkowski, L., Ellis, J.I., Needham, H.R., Pilditch, C.A., 2025. A systematic review and meta-analysis of the cumulative effects of multiple stressors on marine bivalves. Mar. Biol. 172, 96. https://doi.org/10.1007/s00227-025-04671-y.

Sánchez-Lazo, C., Martínez-Pita, I., 2012. Biochemical and energy dynamics during larval development of the mussel *Mytilus galloprovincialis* (Lamarck, 1819). Aquaculture 358–359, 71–78. https://doi.org/10.1016/j.aquaculture.2012.06.021.

van der Schatte Olivier, A., Le Vay, L., Malham, S.K., Christie, M., Wilson, J., Allender, S., Schmidlin, S., Brewin, J.M., Jones, L., 2021. Geographical variation in the carbon, nitrogen, and phosphorus content of blue mussels, *Mytilus edulis*. Mar. Pollut. Bull. 167, 112291. https://doi.org/10.1016/j.marpolbul.2021.112291.

Simon, A., Arbiol, C., Nielsen, E.E., Couteau, J., Sussarellu, R., Burgeot, T., Bernard, I., Coolen, J.W.P., Lamy, J.-B., Robert, S., Skazina, M., Strelkov, P., Queiroga, H., Cancio, I., Welch, J.J., Viard, F., Bierne, N., 2020. Replicated anthropogenic hybridisations reveal parallel patterns of admixture in marine mussels. Evol. Appl. 13, 575–599. https://doi.org/10.1111/eva.12879.

Smolders, R., Bervoets, L., De Coen, W., Blust, R., 2004. Cellular energy allocation in zebra mussels exposed along a pollution gradient: linking cellular effects to higher levels of biological organization. Environ. Pollut. 129, 99–112. https://doi.org/10.1016/j.envpol.2003.09.027.

Solé, M., Kaifu, K., Mooney, T.A., Nedelec, S.L., Olivier, F., Radford, A.N., Vazzana, M., Wale, M.A., Semmens, J.M., Simpson, S.D., Buscaino, G., Hawkins, A., Aguilar de Soto, N., Akamatsu, T., Chauvaud, L., Day, R.D., Fitzgibbon, Q., McCauley, R.D., André, M., 2023. Marine invertebrates and noise. Front. Mar. Sci. 10. https://doi.org/10.3389/fmars.2023.1129057.

de Soto N., Aguilar, Gkikopoulou, K., Hooker, S., Isojunno, S., Johnson, M., Miller, P., Tyack, P., Wensveen, P., Donovan, C., Harris, C.M., Harris, D., Marshall, L., Oedekoven, C., Prieto, R., Thomas, L., 2016. From physiology to policy: a review of physiological noise effects on marine fauna with implications for mitigation. Proc. Meetings Acoust. 27, 040008. https://doi.org/10.1121/2.0000299.

Svavarsson, J., Guls, H.D., Sham, R.C., Leung, K.M.Y., Halldórsson, H.P., 2021. Pollutants from shipping - new environmental challenges in the subarctic and the Arctic Ocean. Mar. Pollut. Bull. 164, 112004. https://doi.org/10.1016/j.marpolbul.2021.112004.

Veillard, D., 2025. Effets multi-omiques sur l'ontogenèse de la moule bleue *Mytilus Edulis* exposée au trafic maritime : approche écophysiologique (phd). Université du Québec à Rimouski, Rimouski.

Veillard, D., Beauclercq, S., Ghafari, N., Arnold, A., Genard, B., Sleno, L., Olivier, F., Choquet, A., Warschawski, D., Marcotte, I., Tremblay, R., 2025a. Molecular evidence of shipping noise impact on the blue mussel, a key species for the sustainability of coastal marine environments. Mar. Ecol. Prog. Ser. 759, 35–50. https://doi.org/10.3354/meps14830.

Veillard, D., Beauclercq, S., Palacios, E., Genard, B., Chauvaud, L., Olivier, F., Marcotte, I., Tremblay, R., 2025b. Metabolomic responses to shipping noise in early life stages of blue mussels, *Mytilus edulis*. J. Exp. Biol. 228, jeb250386. https://doi.org/10.1242/jeb.250386.

Veillard, D., Beauclercq, S., Bianic, M., Genard, B., St-Louis, R., Chauvaud, L., Marcotte, I., Olivier, F., Tremblay, R., 2026. Effect of chemical pollution representative of an industrial port on the embryonic success of the blue mussel, *Mytilus edulis*: a metabolomic approach. Can. J. Zool. https://doi.org/10.1139/cjz-2025-0051.

Viarengo, A., Pertica, M., Mancinelli, G., Palmero, S., Zanicchi, G., Orunesu, M., 1982. Evaluation of general and specific stress indices in mussels collected from populations subjected to different levels of heavy metal pollution. Mar. Environ. Res. 6, 235–243. https://doi.org/10.1016/0141-1136(82)90057-5.

Viarengo, A., Lowe, D., Bolognesi, C., Fabbri, E., Koehler, A., 2007. The use of biomarkers in biomonitoring: a 2-tier approach assessing the level of pollutant-induced stress syndrome in sentinel organisms. Comp. Biochem. Physiol., Part C: Toxicol. Pharmacol. 146, 281–300. https://doi.org/10.1016/j.cbpc.2007.04.011.

Wishart, D.S., Guo, A., Oler, E., Wang, F., Anjum, A., Peters, H., Dizon, R., Sayeeda, Z., Tian, S., Lee, B.L., Berjanskii, M., Mah, R., Yamamoto, M., Jovel, J., Torres-Calzada, C., Hiebert-Giesbrecht, M., Lui, V.W., Varshavi, D., Varshavi, D., Allen, D., Arndt, D., Khetarpal, N., Sivakumaran, A., Harford, K., Sanford, S., Yee, K., Cao, X., Budinski, Z., Liigand, J., Zhang, L., Zheng, J., Mandal, R., Karu, N., Dambrova, M., Schiöth, H.B., Greiner, R., Gautam, V., 2022. HMDB 5.0: the human metabolome database for 2022. Nucleic Acids Res. 50, D622–d631. https://doi.org/10.1093/nar/gkab1062.

Wu, H., Wang, W.-X., 2010. NMR-based metabolomic studies on the toxicological effects of cadmium and copper on green mussels *Perna viridis*. Aquat. Toxicol. 100, 339–345. https://doi.org/10.1016/j.aquatox.2010.08.005.

Xia, J., Wishart, D.S., 2010. MSEA: a web-based tool to identify biologically meaningful patterns in quantitative metabolomic data. Nucleic Acids Res. 38, W71–W77. https://doi.org/10.1093/nar/gkq329.

Supplementary information to:

Stage-specific metabolic responses in blue mussels to marine shipping-related acoustic and chemical stressors

Stéphane Beauclercq[a], Delphine Veillard[b], Richard St-Louis[b], Frédéric Olivier[c,d], Dror E. Warschawski[e], Réjean Tremblay[b] and Isabelle Marcotte[a*]*

[a]Department of Chemistry, Université du Québec à Montréal, P.O. Box 8888, Downtown Station, Montreal, QC, Canada

[b]Institut des Sciences de la Mer de Rimouski, Université du Québec à Rimouski, Rimouski, QC, Canada

[c]Laboratoire de 'Biologie des Organismes et Écosystèmes Aquatiques' (BOREA), Muséum national d'Histoire naturelle, Sorbonne Université, Université des Antilles, Centre National de la Recherche Scientifique, Institut de Recherche pour le Développement-207, CP53, 61 rue Buffon, 75005 Paris, France.

[d]Université Bretagne Occidentale (UBO), CNRS, IRD et Institut Universitaire Européen de la Mer, 29280 Plouzané, France.

[e]Chimie Physique et Chimie du Vivant, CPCV, CNRS UMR 8228, Sorbonne Université, École normale supérieure, PSL University, 75005, Paris, France

*Corresponding authors

Table S1. Number of independent biological replicates (*Larvosonic* cylinders) per developmental stage, treatment, and experimental run.

Stage	Exp.	Ctrl	Low	Med	High	Chem	Chem+Low	Chem+Med	Chem+High
D-larvae	**1**	6	5	5	6	–	–	–	–
Post-larvae	**1**	4	4	6	5	–	–	–	–
Post-larvae	**2**	3	3	1	3	3	3	3	3
D-larvae	**3**	5	–	–	–	6	–	–	–
Post-larvae	**3**	3	3	2	3	3	3	3	3

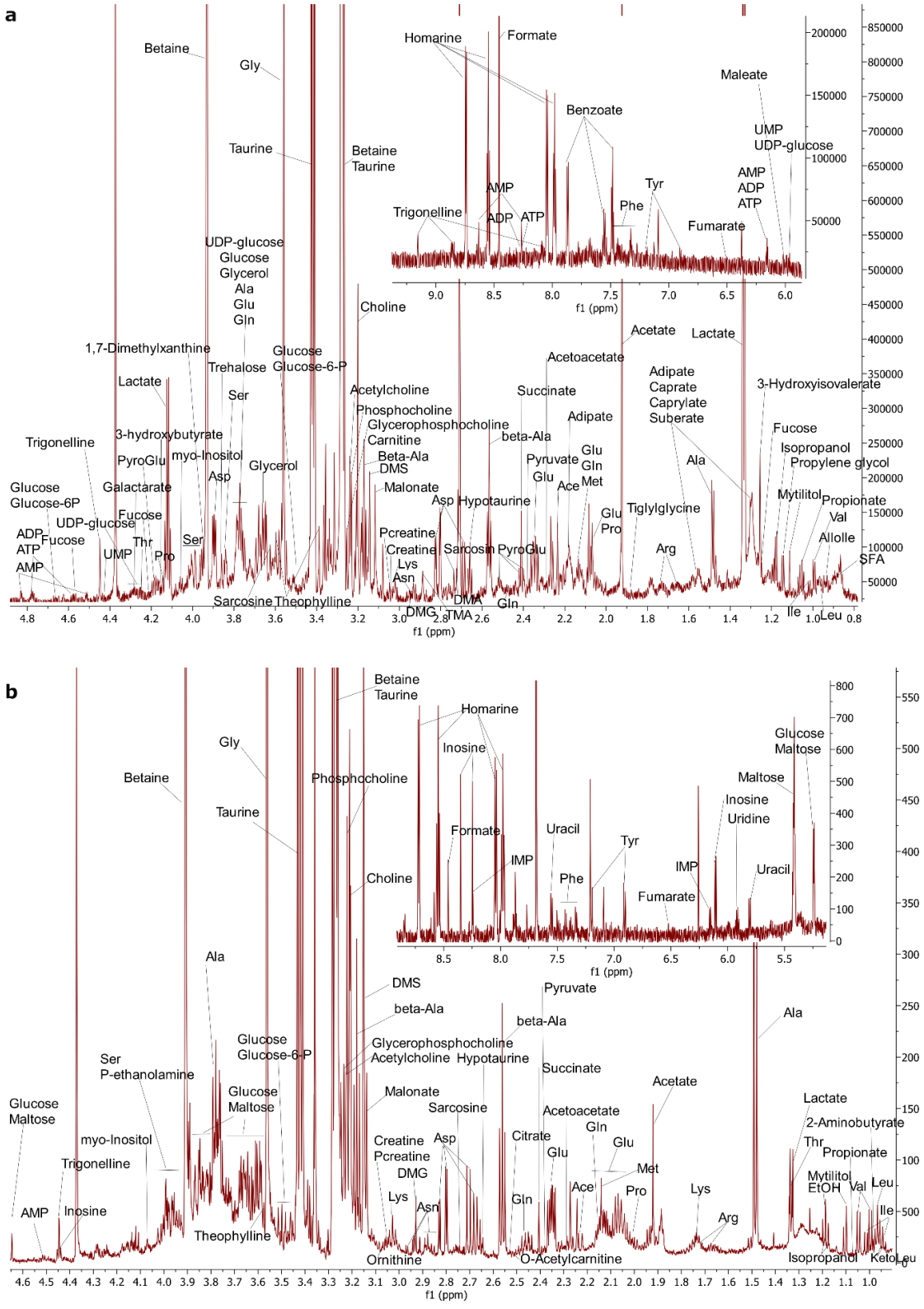

Figure S1. ^{1}H-NMR metabolomic profiles of blue mussel larvae at different developmental stages. Representative ^{1}H-NMR spectra of **(a)** D-larvae (Bruker Avance II+ 800 MHz, 1.7 mm microcryoprobe, NOESYGPPR1D, 64k points, D1 = 5 s, D8 = 80 ms, 16 + 1024 scans, spectral width = 15 ppm) and **(b)** post-larvae (Bruker Avance III 600 MHz, 5 mm RT BBFO probe, NOESYPR1D, 64k points, D1 = 10 s, D8 = 50 ms, 8 + 1024 scans, spectral width = 12 ppm), shown for metabolite identification and illustration purposes only. Spectra were annotated independently of the signal-to-noise filtering (S/N ≥ 3) applied to the analytical dataset; for D-larvae, the spectrum was acquired using acquisition parameters that differed from those used for quantitative analysis. Ace, acetone; DMA, dimethylamine; DMG, dimethylglycine; DMS, dimethyl sulfone; SFA, short-chain fatty acids; TMA, trimethylamine.

Table S2 Contribution and variable importance in projection (VIP) of metabolites included in the OPLS-DA model comparing control and high-noise exposed D-larvae ($R^2Y = 0.97$, $Q^2 = 0.94$, CV-ANOVA = 0.00024). Negative contributions indicate metabolites with higher relative levels in control D-larvae, whereas positive contributions indicate metabolites with higher relative levels in larvae exposed to high acoustic stress (~151 re 1 µPa).

Chemical shift (ppm)	Contribution	VIP	Metabolite
8.550	0.544113	0.826038	Homarine
7.984	-0.193706	0.937309	Homarine
7.564	0.883031	0.823856	Benzoate
4.447	-0.636325	0.648929	Trigonelline
4.067	1.490500	1.060160	Unknown
3.283	-0.101737	0.848095	Taurine
3.226	-1.098720	0.995658	Phosphocholine
3.181	2.183740	1.225470	β-Alanine
3.173	0.784828	0.984830	β-Alanine
2.880	-0.689540	1.298660	Unknown
2.814	1.301360	1.211070	Aspartate
2.692	1.845590	1.280560	Aspartate
2.565	2.487120	0.651667	β-Alanine
2.519	1.075700	0.960344	Pyroglutamate
2.272	2.162030	1.135860	Acetoacetate
2.244	2.397440	0.885600	Unknown
2.147	0.575761	0.971696	Glutamate, Glutamine
1.487	1.249750	0.935132	Alanine

Table S3. Contribution and variable importance in projection (VIP) of metabolites included in the OPLS-DA model comparing control and chemically exposed D-larvae ($R^2Y = 0.99$, $Q^2 = 0.98$, CV-ANOVA = 5.89×10^{-5}). Negative contributions indicate metabolites with higher relative levels in control D-larvae, whereas positive contributions indicate metabolites with higher relative levels in D-larvae exposed to chemical pollution.

Chemical shift (ppm)	Contribution	VIP	Metabolite
9.135	-0.917132	0.847495	Trigonelline
8.2765	1.4066	1.06681	AMP, ADP
7.954	0.891138	0.794616	UDP-N-Acetylglucosamine
7.771	-0.430652	0.764883	Unknown
3.896	1.28601	0.994417	Unknown
3.749	1.68999	1.15193	Unknown
3.5215	0.849782	0.777647	Unknown
3.424	1.25714	1.00077	Taurine
3.3635	-1.76543	1.11613	Hypotaurine
3.3465	-1.76453	1.12148	Hypotaurine
3.152	-1.13577	0.940987	Dimethyl sulfone
3.032	-0.891765	0.868658	Creatine, Creatine phosphate
2.972	2.14744	1.23204	Glutathione
2.925	-1.16381	0.999805	Unknown
2.814	1.79038	1.13592	Aspartate
2.692	1.12988	0.94515	Aspartate
2.6565	-2.10254	1.24095	Hypotaurine
2.4685	1.02401	0.953508	Glutamine
2.3525	1.53574	1.03167	Glutamate
2.26	-2.08742	1.25092	Unknown
1.4865	0.923352	0.813507	Alanine
1.333	-0.524316	0.648395	Lactate

Table S4. Contribution and variable importance in projection (VIP) of metabolites included in the OPLS-DA model comparing control and high-noise exposed post-larvae (R^2Y = 0.98, Q^2 = 0.90, CV-ANOVA = 7.9687×10^{-5}). Negative contributions indicate metabolites with higher relative levels in control post-larvae, whereas positive contributions indicate metabolites with higher relative levels in larvae exposed to high acoustic stress (~151 re 1 µPa).

Chemical shift (ppm)	Contribution	VIP	Metabolite
4.1194	0.0749167	0.579658	Unknown
4.1072	0.263936	0.502160	Unknown
3.7586	-1.17281	1.260170	Glutamate
3.7525	-1.36907	1.315740	Glutamate
3.7455	-1.89787	1.462590	Glucose, Maltose, Glutamate
3.7416	-0.762142	1.095370	Acetylcholine
3.6984	0.299398	0.790006	Maltose
3.6869	-0.321127	0.898513	Unknown, Mannitol, Maltose
3.6318	0.820752	1.084820	Maltose
3.5142	0.787229	1.114480	Glucose, Unknown
3.5045	0.233515	0.860480	Glucose
3.4564	0.868407	1.031760	Glucose
3.4207	1.19008	1.225910	Taurine, Betaine
3.3524	0.95315	1.126360	Hypotaurine
3.2533	0.330853	0.836557	Glucose
3.2263	0.73378	1.080940	Acetylcholine
3.2202	0.137956	0.801413	Phosphocholine
3.1793	-0.229121	0.911221	β-Alanine
3.1497	0.723147	1.087400	Dimethyl sulfone
2.9379	0.201781	0.795700	Asparagine, Unknown
2.9128	1.01855	1.014220	Unknown
2.8914	-0.308829	0.912269	Asparagine
2.561	-0.058483	0.856031	β-Alanine
2.463	-0.775715	0.806584	Glutamine
2.4054	-0.442893	0.992816	Succinate
2.2881	-0.159904	0.822535	Acetoacetate
2.2218	-0.744848	1.137280	Unknown
2.0546	-0.912105	0.900130	Pyroglutamate
1.8855	1.28884	1.186450	Unknown
1.4836	-0.422409	0.855155	Alanine
1.3443	-1.03973	0.985488	Threonine
1.0024	-0.657427	1.033390	Valine
0.9547	-0.465914	0.991039	Isoleucine, Leucine

Table S5. Contribution and variable importance in projection (VIP) of metabolites included in the OPLS-DA model comparing control and chemically exposed post-larvae ($R^2Y = 0.99$, $Q^2 = 0.97$, CV-ANOVA = 8.46×10^{-5}). Negative contributions indicate metabolites with higher relative levels in control post-larvae, whereas positive contributions indicate metabolites with higher relative levels in D-larvae exposed to chemical pollution.

Chemical shift (ppm)	Contribution	VIP	Metabolite
4.0276	0.44341	0.755555	AMP
4.0138	1.59999	1.10178	Unknown
4.0067	1.64175	1.21973	Unknown
3.9486	-0.135642	0.811748	Serine
3.9419	-0.282911	0.904148	Serine
3.9367	-0.00140732	0.81087	Creatine, Serine
3.8966	-0.159339	0.436233	Aspartate
3.8374	0.141067	0.668733	Serine
3.8317	-0.319267	0.853941	Unknown
3.7455	-0.514604	0.639484	Acetylcholine
3.7263	-0.735774	0.845926	Dimethylglycine
3.692	-0.633011	0.722827	Unknown
3.6869	-0.561217	1.15468	Unknown
3.6274	1.50582	1.11952	Myo-Inositol
3.6114	1.14434	1.11971	Maltose
3.5978	1.36953	1.39371	Phosphocholine
3.5142	2.68127	1.11934	Glucose
3.5045	1.60368	1.10358	Unknown
3.4969	1.52051	1.05844	Glucose
3.4882	1.10786	0.84813	Unknown
3.376	1.21831	0.89671	Unknown
3.3472	0.80507	0.837046	Proline
3.2202	-0.2288	1.09801	Unknown
3.205	0.199923	1.20731	Choline
3.1346	-0.945603	0.718251	Malonate
3.1241	1.23541	1.09885	Phenylalanine
3.1165	1.93661	1.15204	Unknown
3.0605	-1.08219	1.25108	Unknown
3.0302	1.8531	0.811861	Lysine
2.9379	1.90631	1.26621	Asparagine
2.7112	-0.0485874	0.370198	Aspartate
2.6885	1.64737	1.22312	Citrate
2.6414	-0.591754	0.890809	Hypotaurine
2.4054	0.433307	0.656327	Succinate
2.2881	1.33661	1.12172	Acetoacetate
2.2607	1.31322	1.07416	Unknown
2.0546	0.495887	0.730861	Pyroglutamate
1.5151	1.92158	1.2705	Unknown

1.5031	1.15953	1.0794	Unknown
1.1115	1.35943	1.03648	Unknown
0.9901	1.40836	1.17359	Valine
0.9547	1.45009	1.14974	Isoleucine, Leucine
0.9427	1.35223	1.04121	Isoleucine

Table S6. Contribution and variable importance in projection (VIP) of metabolites included in the OPLS-DA model comparing control and sequentially exposed to chemical during embryogenesis and high-noise during metamorphosis (R^2Y = 0.99, Q^2 = 0.98, CV-ANOVA = 2.25×10^{-6}). Negative contributions indicate metabolites with higher relative levels in control post-larvae, whereas positive contributions indicate metabolites with higher relative levels in post-larvae exposed to high acoustic stress (~151 re 1 µPa) and chemical pollution.

Chemical shift (ppm)	Contribution	VIP	Metabolite
4.1194	0.928214	0.797267	Lactate
3.9486	-0.898012	1.0069	Serine
3.8472	-0.438566	0.879991	Serine
3.8426	-0.793566	0.936046	Serine
3.7455	-1.78215	1.11108	Acetylcholine
3.7416	-1.70846	1.1961	Acetylcholine
3.6274	0.92936	0.816621	myo-Inositol
3.6114	0.75934	0.832361	Maltose
3.6035	1.35353	1.08795	Phosphocholine
3.5978	1.30376	1.06405	Maltose
3.593	1.23213	1.08743	Threonine
3.3874	1.11233	1.00213	Unknown
3.376	1.82233	0.858068	Unknown
3.3692	1.48048	1.10005	Unknown
3.3524	0.873404	0.935752	Hypotaurine
3.3472	1.70723	0.953227	Proline
3.2353	0.561822	1.13322	Carnitine
3.1793	-0.610487	1.04701	β-Alanine
3.1241	1.8361	1.04295	Phenylalanine
3.1165	1.62311	1.21999	Unknown
2.9379	1.31549	0.993802	Asparagine
2.6885	0.806002	0.88643	Citrate
2.6551	-0.627239	0.976385	Hypotaurine
2.6414	-0.90417	1.03359	Unknown, Methionine
2.561	-0.63023	1.12121	β-Alanine
2.4054	1.76264	0.97946	Succinate
1.0974	1.60552	1.06535	Mytilitol
0.9901	0.843154	0.851223	Valine
0.9427	0.812849	0.783742	Isoleucine